Social Network Addiction*

Tin Cheuk Leung† Wake Forest University

Koleman Strumpf‡ Wake Forest University

Tsz-Nga Wong§ Federal Reserve Bank of Richmond

Preliminary, Do Not Cite
March 2025

Abstract

Recent work has attempted to measure the addictive nature of social network. We contribute to this literature in two key ways. First, we develop a search model that incorporates (i) rational addiction driven by habit formation, (ii) behavioral addiction influenced by present bias, projection bias, and perception bias, and (iii) network effects mediated by matching on platforms. The latter is particularly important: even in the absence of habit formation or behavioral biases, persistent network activity could arise solely from network effects but be misinterpreted as addiction. Second, we examine the model's testable implications using a new panel dataset with a sufficiently long sampling period to mitigate potential censoring bias. Leveraging exogenous shocks through a graph of friends, we find evidence of network effects but little support for behavioral biases. Having controlled for the network effects, our long panel data reveals that social-network addiction is short-lived, with its effects largely dissipating within a year. The strength of network effects highlights potential regulatory implications.

JEL Classification: D12, D90, D91, L82, L86, O33

Keywords: Digital Addiction, Social Media, Network Effect, Search Model, Habit Formation, Self-control

*We would like to thank Babur De los Santosm, Matthew Lewis, Christy Zhou, and seminar participants at Clemson for valuable comments. The views expressed here are those of the authors and should not be interpreted as those of the Federal Reserve Bank of Richmond or the Federal Reserve System.

†Contact: Department of Economics, Kirby Hall, Wake Forest University, Box 7505, Winston-Salem, NC 27109. Email: leungtc@wfu.edu

‡Email: strumpks@wfu.edu

§Email: russell.wong@rich.frb.org

1 Introduction

Social media addiction is increasingly recognized as a growing concern. According to a recent Pew Research Center study (Pew Research Center, 2024), nearly one-third of U.S. adults say they are "almost constantly" online, with young adults reporting even higher rates of social media engagement. As platforms compete for user attention, concerns about excessive consumption and its potential consequences—ranging from reduced productivity to negative mental health outcomes—have intensified. Yet, measuring the extent of social media addiction remains challenging, particularly due to the interplay between individual habits and network effects.

This paper develops a tractable dynamic model of social network addiction that accounts for both rational and behavioral addiction while incorporating peer effects in a social network. Unlike standard rational addiction models, our framework introduces habit formation alongside three key behavioral biases—present bias, projection bias, and perception bias. Additionally, we integrate social network effects, where the utility of social media use depends on the activity of one's peers. The model provides closed-form comparative statics, yielding testable implications that allow us to empirically distinguish between rational and behavioral addiction, and network-driven persistence.

Empirically, we leverage a rich, long-panel dataset tracking individual social media app usage and mobility throughout 2020. By combining app usage data from Global Wireless Solutions, county-level mobility data from Google, and the Facebook Social Connectedness Index (SCI), we construct a proxy for an individual's social network. This dataset enables us to test the theoretical model's predictions by examining the persistence of social media use, the role of peer effects, and the impact of mobility shocks induced by COVID-19 lockdowns. Our findings suggest that social media addiction is relatively short-lived, with persistence largely dissipating within a year. We also document strong peer effects—an individual's social media usage increases when their network is more engaged.

A key result of our empirical analysis is that we can reject strong behavioral biases as the primary driver of social media addiction. While habit formation and peer effects play significant roles, we find little evidence supporting time-inconsistent behavior, such as extreme present bias. These findings have important policy implications. If social media

consumption is driven in part by network externalities, individuals may fail to internalize how their usage encourages others to engage, leading to over-consumption. This suggests that interventions—such as usage caps, pricing adjustments, or regulatory measures—may be justified even in the absence of behavioral biases.

Our study builds on prior work on rational and behavioral addiction models, extending the framework to account for social network effects. By integrating a dynamic model with a unique long-panel dataset and leveraging network-level variation, we provide new insights into the nature of social media addiction. Understanding these dynamics is crucial for policymakers, platform designers, and researchers concerned with the broader societal implications of digital consumption.

The remainder of the paper is as follows. Section 2 reviews the related literature. We build a model of social network addiction in Section 3. We then describe the data in Section 4, and then discuss our main analysis and present our empirical results in Section 5. The last section concludes.

2 Literature

Our framework builds on the decision-theoretic rational addiction model, which presumes agents are forward looking when they make dynamic consumption choices. This is the benchmark model for goods such as smoking where the benefit of consumption has state dependence, for example where past consumption influences current enjoyment of consumption through an additive addiction stock. Becker and Murphy (1988) model individuals as committing to a dynamic consumption plan, which might include becoming addicted and later cessation, that maximizes lifetime utility. Fundamental to this model is that individuals anticipate future consequences of their current actions, and so future environmental changes can influence current behavior. For example, anticipated future price changes can reduce consumption today and this effect will be larger for permanent rather than transient price changes.

Later papers include behavioral modifications to this rational addiction model. Laibson (1997) and Gruber and Köszegi (2001) allow forward looking individuals to have a present bias which leads to time inconsistent preferences. For example, individuals may

plan to cease consumption of the addictive good in the future, but when that time comes they cannot follow-through on their plan. Individuals differ in whether they do (sophisticates) or do not (naifs) understand they have this self-control problem.Loewenstein, O'Donoghue, and Rabin (2003) allows individuals to have a projection bias. For example, individuals may be inattentive if they fail to recognize the likelihood of becoming addicted when they make current decisions. Bernheim and Rangel (2004) consider individuals who enter modes in which they can make mistakes in their consumption choices, and environmental conditions as well as past use shape how likely they are to enter such "hot" states. O'Donoghue and Rabin (1999) allow individuals to have projection bias in the sense that they are naive to recognize that they have present bias or projection bias. Allcott, Gentzkow, and Song (2022) consider a special case where individuals are naive about their present bias but not about their project bias. In these models the fully rational model is a limiting case in which the behavioral anomalies disappear.

Our contribution lies in incorporating social network effects into an addiction model while accounting for behavioral biases. Flow utility depends on the number of friends who also consume the good, a key feature of social media, where engagement depends heavily on the presence of peers. Measuring the role of network effects in social media consumption has important policy implications. Even under full rationality, social media may be overconsumed due to network externalities—individuals do not internalize how their usage encourages others to engage. This negative externality could be addressed through policy interventions such as quantity restrictions or pricing mechanisms. Furthermore, distinguishing between addiction and network-driven persistence is critical, as observational data may confound the two. A shift from a low-usage equilibrium to a high-usage equilibrium could sustain social media engagement even in the absence of addiction, underscoring the importance of incorporating network effects into addiction models.

We are not the first to incorporate social networks into addiction models. Gilo and Tsodikovich (2020) and Reif (2019) examine dynamic addiction to a harmful product among informed individuals who are connected to a network of users. However, these models do not account for the behavioral biases outlined above. Our approach extends this literature by integrating social networks with various cognitive biases to provide a

more comprehensive framework.

Several empirical studies examine addiction in the context of social media, though their measures of social network size remain relatively crude. For example, Allcott, Gentzkow, and Song (2022) and Somasundaram, Zimmermann, and Duc (2020) do not control for individual's social network size in their estimation of social media/mobile phone addiction. Kwon et al. (2016) use the total number of users on Facebook and Anipang (a social gaming platform) as proxies for social network size, without considering the actual structure of each individual's network. In contrast, our approach incorporates a more refined measure of social connectedness, allowing for a more precise estimation of network effects on addiction.

We will estimate a dynamic behavioral model which allows for social effects. After allowing for these network effects, we will test if individuals are forward looking and time consistent (rational) or instead have behavioral patterns (for example over-weighting the present period).

3 Model of Social Network Addiction

Overview. We consider a stylized version of addiction as a state in which individuals lose decision-making autonomy and are compelled to engage in the addictive activity at the maximum feasible level. Our focus is on the decision-making process of non-addicted individuals, taking into account both the benefits of the activity and the risk of becoming addicted. In the context of social networks, the primary benefit arises from interactions with "friends" on the platform. The intensity of both an individual's own activity and that of their friends increases the likelihood of beneficial interactions but also heightens the risk of addiction. An addicted individual transitions back to a non-addicted state with some exogenous probability, analogous to the depreciation of addiction stock in rational addiction models. Our model's implications are robust to various extensions and alternative environments.

We first consider a model of perfectly rational individuals who optimize their decisions in a forward-looking and time-consistent manner. Similar to models of habit formation, non-addicted individuals recognize how their current choices influence their future well-

being by affecting the probability of transitioning between addiction states.

Next, we introduce behavioral biases, specifically: (i) present bias, which reflects a self-control problem leading to overindulgence in the present activity; (ii) projection bias, which entails a failure to recognize how current activity increases the likelihood of addiction; and (iii) perception bias, which captures individuals' misjudgment of their own self-control limitations.

We demonstrate that these two versions of the model—both incorporating network effects and forward-looking behavior to varying extents—yield distinct empirical predictions regarding comparative statics and responses to changes in the network.

3.1 Baseline Model

Technology. Time runs continuously from 0 to T, as in Becker and Murphy (1988). In our model, agents derive utility from social interactions. Specifically, social interactions occur at arrival rate of $\lambda(x, X)$, where $\lambda(.,.)$ follows the standard matching technology à la Diamond-Mortensen-Pissarides search models. This arrival rate depends on both the agent's own activity on the social network, x, and also his friends' activities, X. Social network (SN) activities are complement if $\frac{\partial^2 \lambda}{\partial x \partial X} \geq 0$ and substitute if $\frac{\partial^2 \lambda}{\partial x \partial X} \leq 0$. We assume that the matching technology is increasing and concave in the agent's activity, i.e., $\frac{\partial \lambda}{\partial x} \geq 0$ and $\frac{\partial^2 \lambda}{\partial x^2} \leq 0$.

Preferences. There is a continuum of agents who are either in state of addicted ($S_t = A$) or non-addicted ($S_t = U$).[1] The preferences of an agent can be written as:

$$\mathcal{U}(S_0) \equiv \max_{\{x_t\}_{t=0}^{T}} \mathbb{E} \int_0^T e^{-rt} \left\{ I_{S_t=U} \left[-h(x_t + m) + \lambda(x_t, X)\, u \right] + I_{S_t=A} \left[-k - h(\bar{x}) \right] \right\} dt,$$

where $h(x_t + m)$ is the disutility of activities, consisting of on-network activity x_t and off-network activities m, e.g. works and commuting, subject to the time constraint $\bar{x}$, u is the utility of each social interaction, and k is the disutility of being addicted to social

[1] Instead of assuming continuous S_t as in Becker and Murphy (1988) and Allcott, Gentzkow, and Song (2022), we represent addiction as a Markov chain with discrete states, $S_t \in \{U, A\}$. As we will see later, this presentation is more tractable for sharper analytical results and testable implications, even without maintaining any assumption on utility, for instance quadratic preferences in Becker and Murphy (1988) and Allcott, Gentzkow, and Song (2022). Furthermore, the discrete-stage model affords us the machinery of standard search models to incorporate social networks directly into individual preferences.

network. The disutility of being addicted, k, captures the net negative welfare effect of social-network addiction to the addicted agents (see Allcott et al. (2020) for more examples). Without loss of generality, we assume that agents who are addicted to social network always max out their social network activity such that $x_a = \bar{x} - m$.

Social interactions also carry the risk of addiction to the social network. In our model, addiction occurs with probability $p \in (0, 1)$ upon each social interaction. Addicted agents eventually recover at an exogenous rate δ. We assume the utility of each social interaction is high enough such that

$$u > p\frac{k + h(\bar{x}) - h(m)}{r + \delta}. \tag{1}$$

As we will see, this assumption guarantees the agent will always have some activity on the social network despite the risk of addiction. In summary, an agent transitions from the addicted state (A) to the non-addicted state (U) at rate δ and from the non-addicted state (U) to the addicted state (A) at rate of $p\lambda(x_t, X)$.

As in typical search models, it is useful to express agents' preferences recursively as $\mathcal{U}(S_0) = I_{S_0=U}V_0^U + I_{S_0=A}V_0^A$, where $V_t^{S_t}$ is the (continuation) value of state S_t given by:

$$V_t^U = \mathbb{E}\left\{\int_t^{\tau\wedge T} -e^{-r(s-t)}h(x_s + m)\,ds + 1_{\tau\leq T}e^{-r(\tau-t)}\left[u + pV_\tau^A + (1-p)V_\tau^U\right]\right\}, \tag{2}$$

$$V_t^A = \mathbb{E}\left\{\int_t^{\tau\wedge T} -e^{-r(s-t)}\left[k + h(\bar{x})\right]ds + 1_{\tau\leq T}e^{-r(\tau-t)}V_\tau^U\right\}, \tag{3}$$

where τ denotes the time at which the individual's next state transitions. Define the (subjective) marginal cost of addiction as

$$\Delta_t \equiv V_t^U - V_t^A.$$

The following lemma states the optimal choice of x_t by the rational agents.

Lemma 1. *The optimal SN activities, $x_t = x_t^*$, that maximizes $\mathcal{U}(S_0)$ are given by:*

$$x_t^* = \arg\max_x \left\{-h(x + m) + \lambda(x, X)(u - p\Delta_t)\right\}, \tag{4}$$

where Δ_t solves the following ordinary differential equation

$$\frac{d\Delta_t}{dt} = [r + \delta + p\lambda(x_t^*, X)]\,\Delta_t - k - h(\bar{x}) + h(x_t^* + m) - \lambda(x_t^*, X)\,u, \text{ where } \Delta_T = 0. \quad (5)$$

Furthermore, we have

$$0 \leq \Delta_t < \frac{u}{p}. \quad (6)$$

In deciding on the optimal SN activity, rational non-addicted agents maximize the expected interaction benefit, $\lambda(x_t, X_t)u$, while weighing the associated costs. These costs include the direct disutility, $-h(x_t+m)$, as well as the marginal cost of addiction, Δ_t. The latter is the feature of forward looking, commonly found in the models of habit formation like Becker and Murphy (1988).

Using Lemma 1, the following proposition summarizes the rational SN activity in term of comparative statics. These sharp results are now available even without maintaining any assumption on the functional forms because modeling addiction as a discrete state, instead of continuum variable, affords us the tractability we need for analytical results.

Proposition 1. ***(Rational Addiction)*** *The comparative statics of the rational agent's activities and his marginal cost of addiction are*

	Addiction prob. dp	*Recovery rate* $d\delta$	*Addiction effect* dk	*Interaction benefit* du	*Matching efficiency* $d\lambda$
dx_t^*	$-$	$+$	$-$	$+$	$+$
$d\Delta_t$	$-$	$-$	$+$	$+$	$+$

Expecting a higher recovery rate (δ) from the addicted state to the non-addicted state, the marginal cost of being addicted (Δ_t) is lower. Then the non-addicted agents increase their SN activity, even though a higher recovery rate only matters in the remote contingency of being addicted. A similar reasoning applies, though in the opposite direction, for the comparative statics of k.

The comparative statics with respect to the SN matching efficiency, λ, is novel because it captures the network effect. On one hand, a higher level of λ increases the chance of interactions, which yield a positive net benefit given $u - p\Delta_t > 0$ from equation (6). On

the other hand, a higher level of λ increases the marginal cost of addiction, Δ_t, because the future value of being non-addicted also rises. Overall, the first effect dominates, leading to an increase in SN activity. A similar reasoning applies to the comparative statics of the addiction probability, p, and of the interaction benefit, b, though in opposite directions.

3.2 Model Extensions

So far, we have presented a stylized model abstract from unnecessary complications and details irrelevant to empirical observations. The insights continue to hold robustly in the following extensions: the optimal activity, x_t^*, is given by the solution to equation (4) after modifying (5).

Other factors. In the baseline model, the intensity of SN activity fluctuates over time due to an individual's transitions between the addicted and non-addicted states. In Appendix A.2.1, we demonstrate that Proposition 1 remains valid even when incorporating additional time-varying factors, such as m_t and X_t, which further influence the dynamics of SN activity. In this extended framework, the parameters m and X in equations (4) and (5) are replaced with their time-dependent counterparts, m_t with X_t respectively.

Activity choice of the addicted. We have assumed that addicted agents do not have control over their SN activity. This assumption is arguably realistic to some extent, as addiction can impair decision-making. It also allows us to focus on the choices of non-addicted agents, who constitute the majority both in reality and in our dataset, as we will demonstrate. In Appendix A.2.2, we show that Proposition 1 remains valid even when addicted agents are allowed to determine their SN activity, provided they do so under a higher u, which reflects a higher benefit as in the habit formation model.

Cold turkey. Up to this point, we have assumed that the recovery rate δ, which governs transitions from addiction to non-addiction, is exogenous. However, in Appendix A.2.3, we extend the model by allowing addicted agents to engage in "cold turkey" activities that actively increase δ, making recovery partially endogenous. Despite this modification, Proposition 1 continues to hold under a revised version of equation (5), which accounts for the agents' ability to influence their recovery dynamics.

Multiple addiction states. So far, we have analyzed the simplest discrete-state

model with only two states. In Appendix A.2.4, we extend the model where S_t takes multiple values in which $u = u(S_t)$ and $k = k(S_t)$ are increasing in S_t.

Making friends. In Appendix A.2.5, we extend the model by allowing agents to form and lose friendships, making X_t a stochastic process. This modification introduces uncertainty in network effects, as both the number of friends and their activities fluctuate unpredictably over time. Consequently, agents choose their SN activity under a dynamic social environment where their social interactions and influences evolve stochastically.

Network competition. In Appendix A.2.6, we extend the model to incorporate multiple social networks, allowing agents to distribute their activities across different platforms. This extension introduces two opposing effects on addiction. On one hand, multiple networks increase addiction risk as agents face more pathways that could lead to addiction, amplifying their overall exposure to addictive influences. On the other hand, agents' activity on a particular network is diluted as their limited time is spread across multiple networks.

Infinite horizon. Following Becker and Murphy (1988) and Allcott, Gentzkow, and Song (2022), we assume a finite horizon, which inherently limits the possible duration, and hence the marginal cost, of addiction. In Appendix A.2.7, we extend the model to an infinite horizon, removing this constraint. In this case, the terminal condition is replaced with the appropriate transversality condition, ensuring that the agent's optimal decisions remain well-defined over an unbounded time frame. Despite this modification, Proposition 1 continues to hold, demonstrating the robustness of our results under an infinite-horizon setting.

3.3 Incorporating Behavioral Biases

In this section, we show how to use our theoretical framework to encompass a wide range of rational and behavioral models, as special cases. These include the present bias where an agent is undiciplined if he has a self-control problem against overdoing the current activity due to hyperbolic discounting (Laibson, 1997; Gruber and Köszegi, 2001), the projection bias where an agent is inattentive if he fails to recognize the likelihood of becoming addicted when he makes current decision (Loewenstein, O'Donoghue, and Rabin, 2003),

and the perception bias where an agent is naive if he fails to recognize if he is undisciplined or inattentive (O'Donoghue and Rabin, 1999). We follow Allcott, Gentzkow, and Song (2022) to only consider the case where agents are partially naive about his present bias but completely naive about his projection bias.[2]

Consider the following perception-perfect equilibrium (O'Donoghue and Rabin, 1999) in which agents with behavioral biases choose a biased version of (4):

$$x^*\left(X_t, \Delta_t^0; \gamma, \alpha\right) = \arg\max_x \left\{-(1-\gamma)\, h\left(x + m_t\right) + \lambda\left(x, X_t\right)\left[u - p\left(1-\alpha\right)\Delta_t^0\right]\right\}, \quad (7)$$

where Δ_t^s is the marginal cost of addiction at time $t+s$ perceived at time t that solves

$$\begin{aligned}
\frac{d\Delta_t^s}{ds} &= \left(r + \delta + p\tilde{\lambda}_{t,s}\right)\Delta_t^s - k - h\left(\bar{x}\right) + \tilde{h}_{t,s} - \tilde{\lambda}_{t,s}u, \text{ where } \Delta_t^{T-t} = 0; && (8)\\
\tilde{h}_{t,s} &= h\left(\tilde{x}_{t,s}^* + m_{t+s}\right); && (9)\\
\tilde{\lambda}_{t,s} &= \lambda\left(\tilde{x}_{t,s}^*, X_{t+s}\right); && (10)\\
\tilde{x}_{t,s}^* &= x^*\left[X_{t+s}, \Delta_t^s; (1-\eta)\gamma, 0\right]. && (11)
\end{aligned}$$

In this model, the present bias is captured by $\gamma \geq 0$ which enables the model to reflect scenarios where agents experience self-control issues. The projection bias is captured by $\alpha \in [0,1]$ which controls the extent to which agents mis-predict the addiction risk. The perception bias is incorporated in the perceived marginal cost of addiction, Δ_t^s, which evolves under the (equilibrium) prediction $\tilde{x}_{t,s}^*$ where $\eta \in [0,1]$ is the parameter of perception bias.

Predicted and actual activities differ, i.e., $\tilde{x}_{t,s}^* \neq x^*\left(X_{t+s}, \Delta_{t+s}^0; \gamma, \alpha\right)$, due to naivete about present bias and projection bias, as well as misprediction of addiction risk. If we shut down the network effect, then our model is simply the continuous-time version of Allcott, Gentzkow, and Song (2022) with Markov states.[3]

The following proposition summarizes the behavioral SN activity in term of compar-

[2]Our results continue to hold if agents are naive about his present bias and projection bias to any different degrees.

[3]To see the parallel between our model and Allcott, Gentzkow, and Song (2022), compare our equation (7) with their equation (2). They assume linear temptation benefit, γx_t. In our model, the temptation comes from lower perceived disutility of activity by a factor γ. Also, Allcott, Gentzkow, and Song (2022) focus on the binary case of perception bias where η is either 0 or 1.

ative statics.

Proposition 2. ***(Behavioral Addiction)*** *The comparative statics of the behavioral agent's activities and his marginal value of addiction are*

	Present bias $d\gamma$	*Projection bias* $d\alpha$	*Perception bias* $d\eta$
dx_t^*	$+$	$+$	$-$
$d\Delta_t^s$	$-$	0	$+$

The logic behind the effect of projection bias on SN activity is straight-forward. On one hand, a higher level of projection bias, α, increases the intensity of the current activity (captured in equation 7) because the agents fails to recognize the associated higher likelihood of becoming addicted. On the other hand, a higher α has no effect on the marginal cost of addiction, Δ_t. It is because the projection bias only affects his assessment of remaining non-addicted, but not his prediction of his future activities, which determines the marginal cost of addiction. Thus, only the first effect is present, leading to an increase in SN activity.

The other comparative statics are novel because it is often challenging to derive analytical results in the standard models of behavioral biases, for example Allcott, Gentzkow, and Song (2022). For the case of present bias, on one hand, a higher level of γ, reduces the perceived disutility of SN activity. On the other hand, an agent with a higher γ also predicts a path of more severe indulgence in future SN activities. Thus, he expects a lower value of remaining non-addicted, hence the marginal cost of addiction decreases. Thus, the two effects align in the same direction, leading to an increase in SN activity.

The model predicts that a higher level of perception bias, η, *decreases* the intensity of SN activity. The key mechanism behind this result is that a higher η actually decreases the perceived marginal cost of addiction, Δ_t^s. Recall that an agent with perception bias fails to recognize their own lack of self control such that he perceives his future self more "rational" than he is. In particular, a higher η represents a greater underestimation of their self-control limit, perceiving it as $(1-\eta)\gamma$ instead of his true limit γ. As a result, the agent expects to maintain a path of less overindulgence in future SN activities, considering himself closer to the higher value achieved by the rational agents. Consequently, he

expects a higher value of being non-addicted and the perceived marginal cost of addiction increases, leading the agent to reduce SN activity.

3.4 Measuring the Forward-looking Mechanism

The forward-looking mechanism in the decision making mediates via the marginal cost of addiction, Δ_t. Although we cannot directly observe Δ_t in the data, we can observe some shocks ε that predicts SN friends' future activities, which will also shift Δ_t, Thus, we can use ε_t as a proxy for Δ_t. In this section, we formally establish the link between ε_t and Δ_t.

Suppose there exists a shock ε_t to SN friends at t such that their activities in the future are given by

$$X^{\varepsilon}_{t+s} = X_{t+s} + \beta_s \varepsilon_t.$$

In other words, the sequence $\{\beta_s\}$ is the impulse response function to X_t. Define $\Delta^s_{\varepsilon,t} \equiv \frac{\partial \Delta^s_t}{\partial \varepsilon_t}$, i.e., the impulse response function to the marginal cost of addiction, Δ^s_t.

Proposition 3. ***(Impulse Response)*** *$\Delta^s_{\varepsilon,t}$ solves the following ODE*

$$\frac{d\Delta^s_{\varepsilon,t}}{ds} = \left(r + \delta + p\tilde{\lambda}^s_t\right)\Delta^s_{\varepsilon,t} - \beta_s\left(u - p\Delta^s_{\varepsilon,t}\right)\left[\tilde{\lambda}^s_{X,t} - \frac{(1-\eta)\,\gamma}{1-(1-\eta)\,\gamma}\tilde{\lambda}^s_{x,t}\frac{\partial x^*_{t,s}}{\partial X_{t+s}}\right],$$

where $\Delta^{T-t}_{\varepsilon,t} = 0$ and its solution is given by

$$\Delta^0_{\varepsilon,t} = \int_0^{T-t} e^{-\int_0^s r+\delta+p\tilde{\lambda}^\tau_t d\tau}\beta_s\left(u - p\Delta^s_{\varepsilon,t}\right)\left[\tilde{\lambda}^s_{X,t} - \frac{(1-\eta)\,\gamma}{1-(1-\eta)\,\gamma}\tilde{\lambda}^s_{x,t}\frac{\partial x^*_{t,s}}{\partial X_{t+s}}\right]ds.$$

The shock ε_t affects the future activities of SN friends X_{t+s} at the marginal factor β_s. Proposition 3 states that $\Delta_{\varepsilon,t}$ represents the present value of two future flows, discounting at the rate $r + \delta + p\tilde{\lambda}^s_t$. The first flow captures the *direct positive* effect of X_{t+s} on the perceived arrival rates of social interactions in the future, $\tilde{\lambda}^s_t$, captured by $\tilde{\lambda}^s_{X,t}$. This flow is positive to Δ_t, because a higher arrival rate directly increases the preceived value of being non-addicted, thereby raising the marginal cost of addiction.The second flow captures the *indirect negative* effect of X_{t+s} on $\tilde{\lambda}_{t+s}$ via the agent's own activity, $\frac{\partial x^*_{t+s}}{\partial X_{t+s}}$, under the influence of perception bias, $(1-\eta)\gamma$. This flow is negative to the marginal cost of addiction, Δ_t, because an agent with perception bias expects higher intensity in the

future than is optimal, following the reasoning outlined after Proposition 2. Consequently, an increase in friends' future SN activity induces the agent to engage in even higher future activity, deviating further from the optimal level and reducing the value of being non-addicted. As a result, Δ_t increases.

Proposition 3 will be useful to establish the following testable implications.

3.5 Testable Implications

To derive testable implications, consider the first-order condition of (7):

$$h'\left(x_t^* + m_t\right) = \lambda_x\left(x_t^*, X_t\right)\left(\frac{u}{1-\gamma} - p\frac{1-\alpha}{1-\gamma}\Delta_t^0\right), \text{ if } x_t^* + m_t < \bar{x}. \tag{12}$$

In the data we observe X_t, m_t and ε_t. The following proposition summarizes their first derivatives and cross derivatives.

Proposition 4. *(**Testable Implications**) The comparative statics with respect to X_t, m_t and ε_t are given as follows:*

a. $\frac{\partial x_t^*}{\partial X_t} = \lambda_{xX,t} / \left[\frac{(1-\gamma)h_t''}{u-p(1-\alpha)\Delta_t} - \lambda_{xx,t}\right]$;

b. $\frac{\partial x_t^*}{\partial m_t} = -1 / \left[\frac{1-\gamma}{u-p(1-\alpha)\Delta_t} - \theta_t\right]$;

c. $\frac{\partial^2 x_t^*}{\partial m_t \partial X_t} = -\left(\frac{\partial x_t^*}{\partial m_t}\right)^2\left(\theta_{X,t} + \theta_{x,t}\frac{\partial x_t^*}{\partial X_t}\right)$;

d. $\frac{\partial x_t^*}{\partial \varepsilon_t} = -\frac{p(1-\alpha)\Delta_{\varepsilon,t}}{[u-p(1-\alpha)\Delta_t]^2}\frac{h_t'}{h_t''}\frac{\partial x_t^*}{\partial m_t}$;

e. $\frac{\partial^2 x_t^*}{\partial X_t \partial \varepsilon_t} = -\frac{p(1-\alpha)\Delta_{\varepsilon,t}}{[u-p(1-\alpha)\Delta_t]^2}\left[\frac{h_t'}{h_t''}\frac{\partial^2 x_t^*}{\partial m_t \partial X_t} + \frac{\partial h_t'/h_t''}{\partial x}\frac{\partial x_t^*}{\partial X_t}\frac{\partial x_t^*}{\partial m_t}\right]$,

where $\theta_t \equiv \frac{\lambda_{xx}(x,X_t)}{h''(x+m_t)} < 0$, $\theta_{X,t} \equiv \frac{\partial \theta_t}{\partial X} = \frac{\lambda_{xxX,t}}{\lambda_{xx,t}}\theta_t \leq 0$ *and* $\theta_{x,t} \equiv \frac{\partial \theta_t}{\partial x} \geq 0$.

Using Proposition 4, the model yields several testable implications that provide insights into the network effects, the role of other activities, and the impact of addiction dynamics on social media usage.

First, the derivative $\frac{\partial x_t^*}{\partial X_t}$ helps identify whether network effects are present. A positive derivative, $\frac{\partial x_t^*}{\partial X_t} > 0$, indicates that increased social media usage by friends makes an individual more likely to use social media as well. This contrasts with the absence of network effects, as in Allcott, Gentzkow, and Song (2022), or cases where agents are perfectly myopic, with $\gamma = 1$.

Table 1: Social Network Addiction Model's Testable Implications

Null Hypotheses	Testable Implications	Alternative
H1: no network effect ($\lambda_{xX} = 0$) or perfectly undisciplined ($\gamma = 1$)	$\frac{\partial x_t^*}{\partial X_t} = 0$	$\frac{\partial x_t^*}{\partial X_t} > 0$, see Prop. 4a
H2: linear disutility ($h'' = 0$)	$\frac{\partial x_t^*}{\partial m_t} = 0$	$\frac{\partial x_t^*}{\partial m_t} < 0$, see Prop. 4b
H3: either H1 or H2 is true	$\frac{\partial^2 x_t^*}{\partial m_t \partial X_t} \geq 0$	$\frac{\partial^2 x_t^*}{\partial m_t \partial X_t} < 0$, see Prop. 4c
H4a: perfectly inattentive ($\alpha = 1$)	$\frac{\partial x_t^*}{\partial \varepsilon_t} = 0$	$\frac{\partial x_t^*}{\partial \varepsilon_t} > 0$, see Prop. 4d
H4b: perfectly naive ($\eta = 1$) and partially inattentive ($\alpha \in [0, 1)$)	$\frac{\partial x_t^*}{\partial \varepsilon_t} = -sign(\beta_s)$	$\frac{\partial x_t^*}{\partial \varepsilon_t} = sign(\beta_s)$, see Prop. 4d
H5a: H4a is true given H1 is rejected	$\frac{\partial^2 x_t^*}{\partial X_t \partial \varepsilon_t} = 0$	$\frac{\partial^2 x_t^*}{\partial X_t \partial \varepsilon_t} > 0$, see Prop. 4e
H5b: H4b is true given H1 is rejected	$\frac{\partial^2 x_t^*}{\partial X_t \partial \varepsilon_t} = -sign(\beta_s)$	$\frac{\partial x_t^*}{\partial \varepsilon_t} = sign(\beta_s)$, see Prop. 4e

Second, the curvature of h', as captured by $\frac{\partial x_t^*}{\partial m}$, provides insights into how exogenous changes in other activities influence social media usage. Specifically, if $\frac{\partial x_t^*}{\partial m} < 0$, a reduction in other activities, such as less commuting during lockdowns, would result in increased social media usage. Combining this with the network effect from the first implication, we would expect that during lockdowns, when individuals experience reduced mobility, the network effect intensifies. This is captured by $\frac{\partial^2 x_t^*}{\partial m \partial X_t} < 0$, implying that lower levels of alternative activities amplify the influence of friends' social media usage on an individual's behavior.

Third, when agents are neither perfectly inattentive ($\alpha = 1$) nor perfectly myopic ($\gamma = 1$), the marginal value of addiction, Δ_t, becomes a critical factor. In this case, we would expect $\frac{\partial x_t^*}{\partial \Delta_t} > 0$, as an increase in the perceived value of addiction (i.e. when addiction is less harmful) leads to higher social media usage. By contrast, if agents are fully inattentive or myopic, this derivative would equal zero. Furthermore, this effect is likely to be magnified by the size of the individual's social network. That is, $\frac{\partial^2 x_t^*}{\partial X_t \partial \Delta_t} > 0$, indicating that individuals with larger social networks are more responsive to changes in the marginal value of addiction.

Table 1 summarizes these testable implications which provide a framework for empirically evaluating the interplay between network effects, reduced alternative activities, and the dynamics of addiction in shaping social media usage.

4 Data

This section compiles data to test the implications of the theoretical model in Section 3. We use three primary sources: a balanced panel of app usage data from Global Wireless Solutions, providing individual-level social media usage throughout 2020; county-level mobility data from Google, tracking movement patterns during the COVID-19 pandemic; and the Facebook Social Connectedness Index, measuring social networks at the county level in the United States.

4.1 Apps Usage Data

This study utilizes data from Global Wireless Solutions's (GWS) anonymized, opt-in consumer panel, which provides insights into smartphone engagement. The GWS dataset is built around a panel of participants who have agreed to share their smartphone usage data. Below, we describe the key features and structure of the data used in this research.

The dataset includes basic demographic information for each individual in the panel, such as gender, race/ethnicity, and age. The race/ethnicity categories include White, Black, Hispanic, Asian, or Other, and all panel participants are aged 18 and above.

The GWS dataset tracks all app usage from Android devices on a continuous basis, 24 hours a day, 7 days a week. It includes location data, such as latitude and longitude, which allows for the derivation of individual locations and the calculation of distance traveled per day. This distance traveled measure is useful as it captures how lockdowns impact mobility and commuting time, making it a good proxy for other activities, m, in our model. The dataset also includes timestamp information, which enables the analysis of the intensity and patterns of smartphone engagement.

The primary focus of this study is on data from the year 2020. The dataset includes approximately 20,000 individuals who participated during 2020. Additionally, it features a balanced panel of approximately 2,900 individuals, providing consistent observations across the year.

4.2 COVID-19 Community Mobility Reports

The COVID-19 Community Mobility Reports,[4] published by Google, provide valuable insights into changes in human mobility patterns during the COVID-19 pandemic. These reports are derived from anonymized and aggregated location data from mobile devices, capturing trends in mobility across various categories of activity.

The focus of this study is on county-level mobility trends within the United States. The data tracks changes in mobility across key categories, including retail, grocery stores, parks, workplaces, and residences. By analyzing these categories, the dataset provides a comprehensive view of how mobility patterns shifted in response to the pandemic and related policies.

Beyond its role in measuring mobility shifts, county-level mobility data serves as a useful proxy for the value of addiction in the context of social media usage. After controlling for the social media activity of an individual's friends, a decline in mobility within connected counties due to lockdowns implies that those friends will likely reduce their social media usage in the future. This dynamic affects the perceived cost of addiction, as lower expected future engagement among peers increases the harm associated if case of addiction. Consequently, a decline in network-wide mobility can be interpreted as an decrease in the value of addiction (or more harm in addiction), as individuals face more negative externalities from persistent usage.

The dataset spans from mid-February 2020 to mid-October 2022, covering a period marked by the implementation of lockdowns, gradual re-openings, and other public health measures. The data serves multiple purposes in research. It enables the measurement of the effects of lockdowns and reopening phases on mobility trends, shedding light on behavioral and societal responses to policy changes. Additionally, the dataset facilitates the examination of geographic variation in mobility responses, providing insights into how different counties reacted to the pandemic based on local conditions and policy implementations.

[4] `https://www.google.com/covid19/mobility/`

4.3 Facebook Social Connectedness Index

The Facebook Social Connectedness Index (SCI) measures the intensity of social connectedness between geographic regions using anonymized Facebook friendship networks.[5] The SCI is built upon a snapshot of active Facebook users and their friendship links, providing a novel measure of social interactions across locations.

The SCI between two locations, i and j, is defined as:

$$\text{SCI}_{i,j} = \frac{\text{FB_Connections}_{i,j}}{\text{FB_Users}_i \times \text{FB_Users}_j}$$

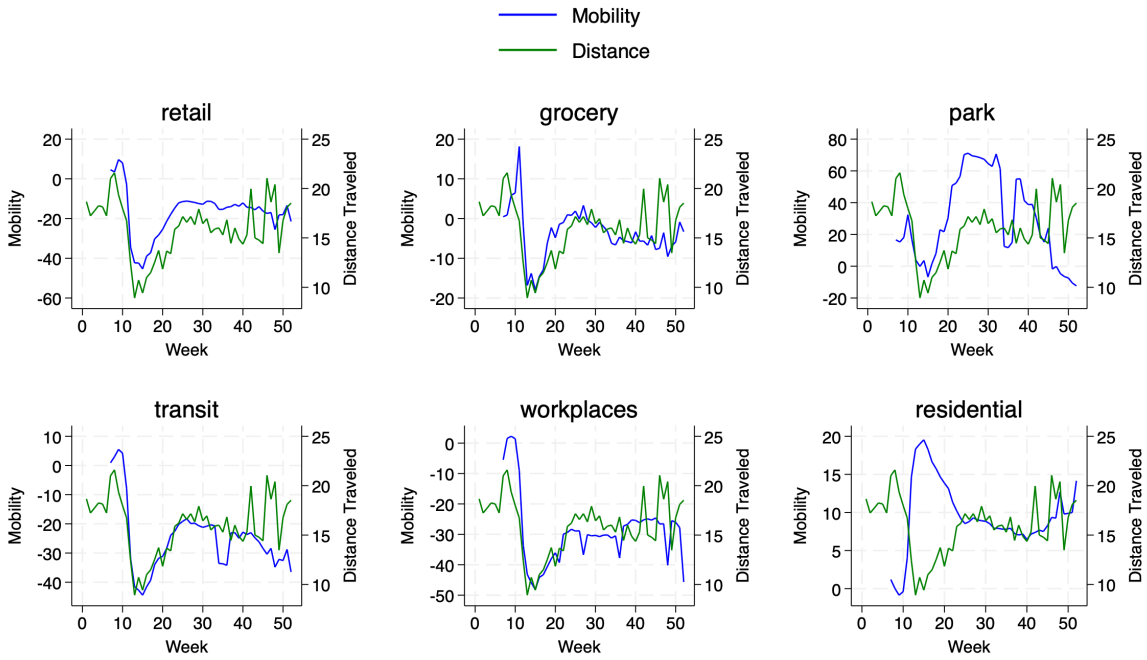
In this formula, $\text{FB_Connections}_{i,j}$ represents the total number of Facebook friendships between users in locations i and j, while $\text{FB_Users}_i, \text{FB_Users}_j$ denote the number of active Facebook users in locations i and j, respectively. To facilitate comparison, the SCI is scaled to range from 1 to 1,000,000,000. This scaling allows the index to represent the relative probability of a Facebook friendship link between users in two locations. For instance, if the SCI between two locations is twice as large as another, users in the first pair of locations are twice as likely to be Facebook friends. The publicly available SCI dataset also includes random noise and rounding to ensure anonymity and protect individual users.

The SCI dataset covers various geographic regions, including pairs of U.S. counties and other administrative areas, and provides a symmetric index where the connection intensity between two locations is equal in both directions. Adjustments are made for connections within the same region to account for users not being connected to themselves. The dataset has been utilized in research to analyze patterns of social connectedness, trade, health outcomes, and geographic mobility, offering valuable insights into the role of social networks in economic and public health contexts.

First introduced and analyzed in Bailey et al. (2018) in the context of U.S. counties, the SCI serves as an important tool for understanding the geographic structure of social networks and their implications for economic and social phenomena.

[5] `https://data.humdata.org/dataset/social-connectedness-index`

Figure 1: Google Mobility and Distance Traveled in 2020



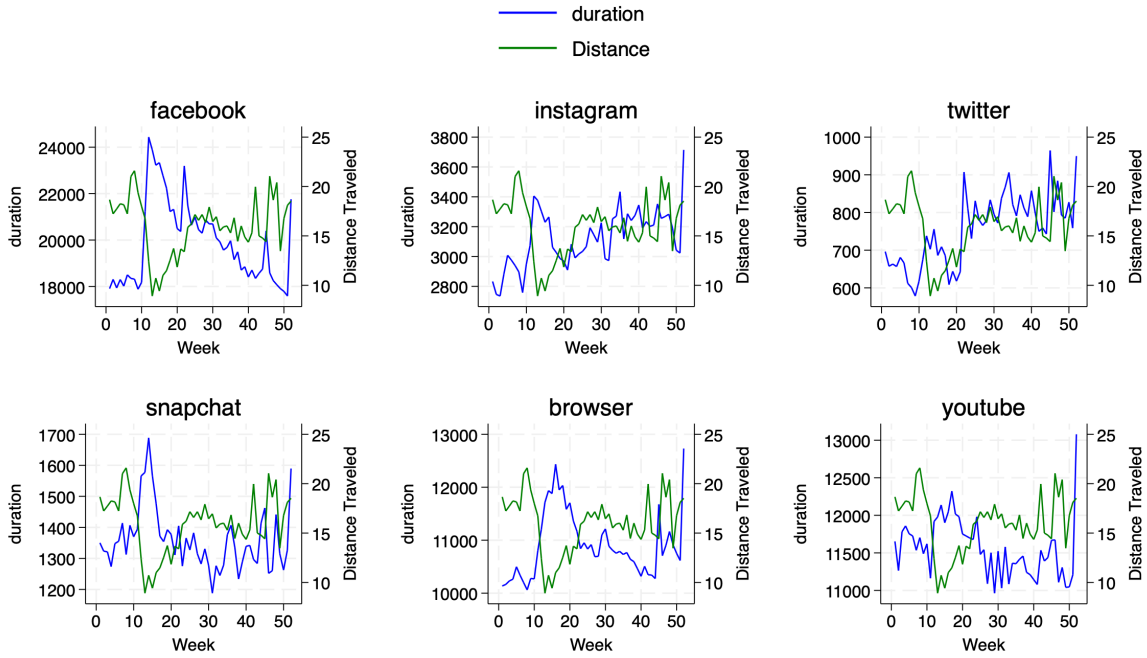
4.4 Summary Statistics

Figure 1 presents a series of subplots that illustrate the relationship between Google mobility measures and the average distance traveled by individuals in the GWS sample over the weeks in 2020. Each subplot depicts the weekly mean of a specific type of Google mobility, including retail, grocery, parks, transit, workplaces, and residential, alongside the average distance traveled by individuals in the GWS dataset.

The trends in most of the Google mobility measures show a positive correlation with individuals' distance traveled. As the average distance traveled increases, so do mobility measures such as retail, grocery, parks, transit, and workplaces. This relationship reflects the intuitive notion that increased mobility in these domains typically involves greater physical movement.

An exception to this pattern is the residential mobility measure. Residential mobility exhibits a negative correlation with individuals' distance traveled. When COVID-19 hit, residential mobility spiked as individuals spent more time at home due to lockdowns and social distancing measures. Over time, residential mobility gradually declined as

Figure 2: App Duration and Distance Traveled in 2020



restrictions eased, and individuals resumed activities outside their homes.

Among the various Google mobility measures, workplace mobility is particularly notable for its consistency and completeness. Unlike other mobility measures, workplace mobility data contains fewer gaps and provides a reliable indicator of weekly activity patterns. For this reason, the analysis that follows primarily relies on the Google workplace mobility measure to assess mobility trends and their relationship with other variables.

Figure 2 illustrates the relationship between the average duration of usage for six social media apps—Facebook, Instagram, Twitter, Snapchat, Browser, and YouTube—and the average individual distance traveled over the weeks in 2020. Each subplot displays the weekly average duration (measured in seconds per week) of app usage alongside the weekly average distance traveled.

As observed in Figure 1, individual mobility dropped significantly once COVID-19 began to impact the United States around week 11 in 2020. This decline in mobility corresponds to a sudden increase in the usage of many social media apps. Facebook, in particular, experienced a dramatic increase in average weekly usage, rising from approx-

imately 18,000 seconds per week (5 hours per week) before COVID-19 to over 24,000 seconds per week (close to 7 hours per week), representing more than a 30% increase. This spike reflects the heightened reliance on social media platforms for communication and entertainment during the initial phases of the pandemic.

Other apps, such as Instagram, Snapchat, and Browser, also exhibited significant increases in usage immediately following the onset of COVID-19, though their increases were less pronounced compared to Facebook. In contrast, Twitter and YouTube showed relatively smaller increases in weekly usage, suggesting a more modest shift in engagement with these platforms during the same period.

Interestingly, while the spike led to high usage of social media for a while which reflects a certain degree of persistence (and hence addiction) in social media usage, the usage of most of these apps, in particular Facebook, Snapchat, and Browser, gradually decreased as lockdowns were phased out, and eventually returned to pre-COVID level by the end of the year.

Table 2 presents the results of regressions examining the relationship between changes in individual mobility and changes in social media app usage. Specifically, we regress the week-to-week change in app usage for individual on the corresponding change in distance traveled by the same individual. The regressions include individual fixed effects, although the results are qualitatively similar when fixed effects are excluded. The goal is to assess whether changes in mobility, particularly during periods such as lockdowns, influence social media usage patterns.

Table 2: Distance Traveled Change on App Usage Change

	(1)	(2)	(3)	(4)	(5)	(6)
	Facebook	Instagram	Twitter	Snapchat	Browser	YouTube
△ Distance Traveled	-2.538***	-0.211	-0.0268	0.0110	-0.392	-1.250***
	(0.361)	(0.134)	(0.0668)	(0.101)	(0.273)	(0.371)
Constant	73.88**	17.95	4.890	4.777	52.69**	30.75
	(33.57)	(12.47)	(6.224)	(9.444)	(25.39)	(34.57)
Observations	146464	146464	146464	146464	146464	146464
Individual FE	Yes	Yes	Yes	Yes	Yes	Yes
R^2	0.00	0.00	0.00	0.00	0.00	0.00

Standard errors in parentheses

* $p < .1$, ** $p < .05$, *** $p < .01$

The table shows that changes in individual mobility are negatively correlated with the usage of most social media apps. The only exception is Snapchat, where the coefficient is

essentially zero, indicating no discernible relationship. Among the platforms, Facebook and YouTube exhibit statistically significant correlations, suggesting that when individual mobility decreases, people tend to use more Facebook and/or YouTube. These findings highlight the prominent role of these platforms during periods of reduced mobility, such as during COVID-related lockdowns.

The analysis uses the full sample for 2020. To ensure robustness, we also restrict the sample to the five weeks before and after the onset of COVID-19 in early March. The results remain consistent with the findings from the full sample, reinforcing the observed relationships between changes in mobility and social media app usage.

Table 3 provides a detailed summary of key variables related to mobility and social media usage, incorporating both individual averages and SCI-weighted measures. The SCI-weighted variable Z for users in county i is calculated as:

$$\bar{Z}_i = \sum_j \frac{\mathrm{SCI}_{i,j} Z_j}{\sum_j \mathrm{SCI}_{i,j}}$$

This metric weights the variable Z by the social connectedness index (SCI) between counties i and j, reflecting the influence of connected regions. For instance, the weighted mobility for a given county is calculated as the sum of the mobility in other counties connected to it, weighted by the Facebook connection strength. Similarly, the weighted social media usage for a county is computed as the sum of the social media usage in other connected counties, also weighted by Facebook connections. The social media usage data for each county is derived from the raw sample of the GWS dataset, without imposing restrictions to a fully balanced panel.

The average distance traveled by individuals per day is approximately 15 miles. This measure highlights the typical mobility pattern of users in the sample during the observed period. The SCI-weighted Google workplace mobility measure is -21.38, indicating that on average, SCI-weighted mobility was 21% lower than the pre-COVID baseline, consistent with the substantial reduction in workplace activity during the pandemic.

In terms of social media usage, Facebook is the most frequently used platform, with an average usage of about 20,000 seconds per week, equivalent to approximately 5.5 hours. This is followed by YouTube (11,000 seconds per week) and browser usage (10,000 seconds

Table 3: Summary Statistics by Apps

	browser	facebook	instagram	snapchat	twitter	youtube	Total
Distance Traveled	15.33	15.33	15.33	15.33	15.33	15.33	15.33
	(106.3)	(106.3)	(106.3)	(106.3)	(106.3)	(106.3)	(106.3)
SCI Weighted Mobility	-21.38	-21.38	-21.38	-21.38	-21.38	-21.38	-21.38
	(7.467)	(7.467)	(7.467)	(7.467)	(7.467)	(7.467)	(7.467)
Weekly Usage (Seconds)	10983.2	20257.5	3189.2	1346.6	782.7	11306.6	7977.7
	(15276.1)	(27733.7)	(10158.9)	(6324.6)	(4991.0)	(26272.2)	(18931.5)
SCI Weighted Usage	2598.6	3376.6	834.9	801.4	454.4	2846.8	1818.8
	(688.4)	(720.4)	(339.2)	(358.4)	(291.9)	(745.2)	(1280.2)
Weighted Usage X Weighted Mobility	-57242.7	-73945.7	-18650.8	-17851.2	-10104.8	-62939.1	-40122.4
	(28933.9)	(35760.3)	(11824.0)	(12071.8)	(8274.5)	(32637.1)	(35002.3)
Weighted Usage X Distance Traveled	37357.4	50123.0	11631.2	11476.1	6157.7	41218.5	26327.3
	(226665.4)	(269366.7)	(53902.9)	(59428.7)	(28339.5)	(227632.0)	(175472.7)

mean coefficients; sd in parentheses

per week). Twitter is the least used social media platform in the sample, with an average of just 780 seconds per week. The SCI-weighted social media usage follows a similar pattern, with Facebook leading and Twitter having the lowest usage. However, SCI-weighted usage is generally lower than the average individual usage, reflecting a dampened effect when accounting for the social connectedness of users across counties.

5 Empirical Specifications and Results

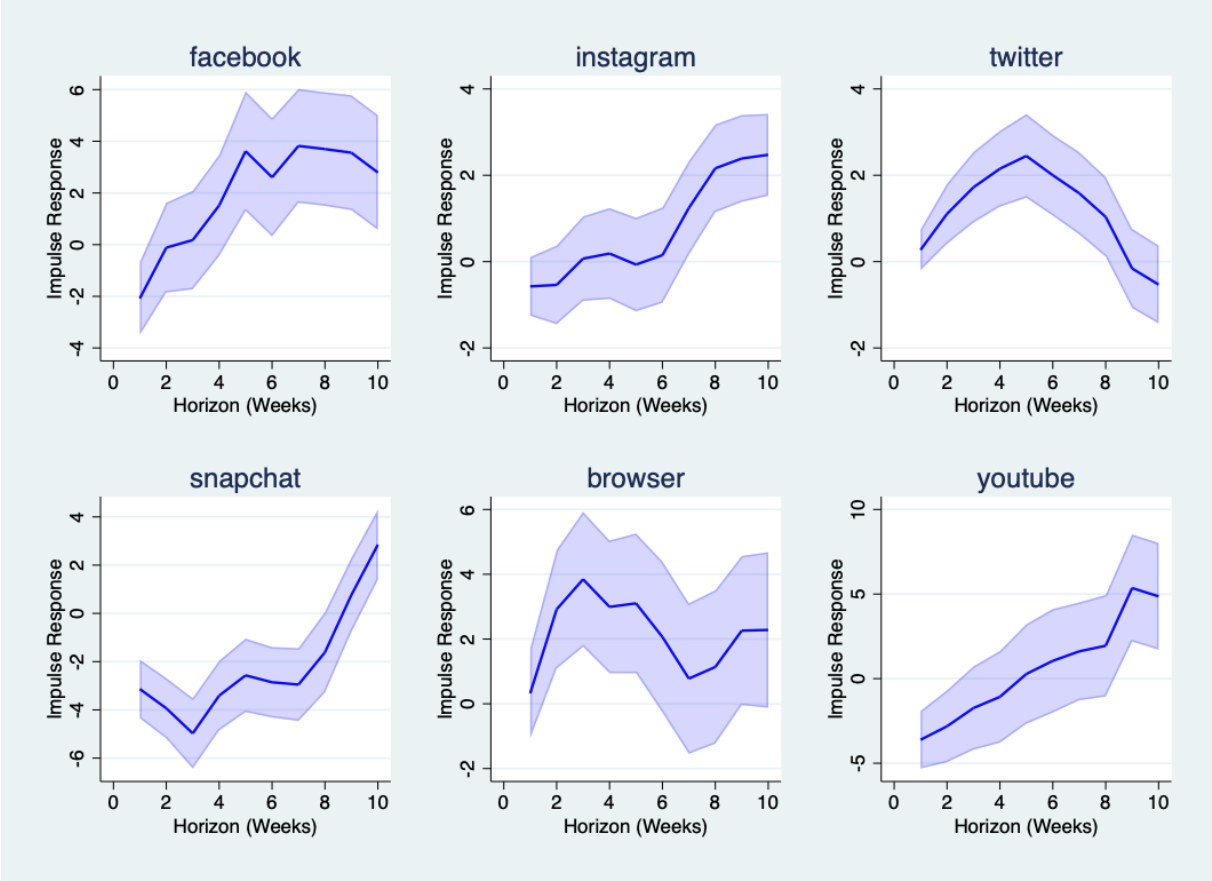
5.1 Impulse Response of Weighted Mobility

In Section 3.4, we demonstrate that a shock to an individual's SN friends at time t can influence their future SN activities, which can be captured through an impulse response function to the marginal value of addiction Δ_t. This is particularly useful for our empirical analysis, as Δ_t is unobservable. Instead, we leverage observable proxies of shocks, such as SCI-weighted mobility which captures the effects of lockdowns across counties, to test the model's implications, particularly those related to changes in Δ_t.

To implement this, we estimate the following local projections regression to obtain the impulse responses of SCI-weighted mobility at t on SCI-weighted social media usage at $t+s$, conditional on the SCI-weighted social media usage at t:

$$\bar{Z}_{it+s}^{usage} = \beta_0^{irf} + \beta_s^{irf}\bar{Z}_{it}^{mobility} + \delta^{irf}\bar{Z}_{it}^{usage} + \phi_i^{irf} + \varepsilon_{it}^{irf}, \tag{13}$$

Figure 3: Impulse Response of Weighted Mobility on Apps Usage



where β_s^{irf} represents the impulse response coefficient on $t+s$. We also demean at the week level to control for the time trend.

The impulse response analysis presented in Figure 3 provides insights into the dynamic relationship between mobility shocks and social media usage. For most social media platforms, the impulse responses are positive, particularly after a lag of two to three weeks. Additionally, the results indicate that for most apps, with the exceptions of Twitter and browser usage (the latter of which has the least "social-network" element among the six apps analyzed here) , the impulse responses tend to grow more positive over time.

This suggests that, conditional on current SCI-weighted social media usage, a lockdown in SN friends' counties—resulting in a reduction in an individual's current weighted mobility—leads to lower social media usage among those friends in the future. This pattern aligns with the theoretical prediction that a decrease in future social media engagement amplifies the harm of addiction, effectively reducing its value, consistent with

$\frac{\partial \Delta_t}{\partial \varepsilon_t} > 0$.

5.2 Empirical Test of Model's Implication

Our main regression specification examines the determinants of individual social media usage, incorporating both individual and social network influences. This regression serves as an empirical test of the testable implications outlined in Section 3.5. Consider the following regression:

$$x_{it} = \beta_1 x_{it-1} + \beta_1 z_{it}^{distance} + \beta_2 \bar{Z}_{it}^{usage} + \beta_3 \bar{Z}_{it}^{usage} \times \bar{Z}_{it}^{mobility} + \beta_4 \bar{Z}_{it}^{mobility} + \beta_5 \bar{Z}_{it}^{usage} \times z_{it}^{distance} + \phi_i + \epsilon_{it}, \tag{14}$$

where x_{it} represents the (demeaned) weekly social media usage of individual i in week t (measured in seconds), and x_{it-1} is the lagged usage, capturing persistence in behavior.[6] To deal with the potential endogeneity in a dynamic panel model, we instrument x_{it-1} using the lagged-lagged usage, i.e. x_{it-2}. ϕ_i is the individual i fixed effects. The variable $z_{it}^{distance}$ denotes the (demeaned) average daily distance traveled by individual i during week t, controlling for mobility constraints that influence time spent on social media. This variable allows us to test whether $\frac{\partial x_t^*}{\partial m} < 0$, implying that we expect $\beta_1 < 0$.

The term $\bar{Z}_{it}^{usage}$ is the (demeaned) SCI-weighted social media usage of individuals connected to i, based on the assumption that all individuals in the same county share the same social network. Since increased social media usage by friends is expected to encourage an individual to use social media more, i.e., social network activities are complement: $\frac{\partial x_t^*}{\partial X_t} > 0$, we anticipate $\beta_2 > 0$. Also, because our model predicts that lower levels of alternative activities would amplify the influence of the social network, i.e. $\frac{\partial^2 x_t^*}{\partial m \partial X_t} < 0$, we expect $\beta_5 < 0$.

Finally, $\bar{Z}_{it}^{mobility}$ represents the (demeaned) SCI-weighted workplace mobility of connected individuals, capturing the broader mobility patterns within the network. As explained earlier, this variable serves as a proxy for the value of addiction in the context of social media usage after controlling for the social media activity of an individual's friends. According to the testable implications of the model, we expect that, if agents are neither

[6] The variables in this regression are all demeaned to control for the time effect.

perfectly inattentive nor perfectly myopic, an increase in the perceived value of addiction would lead to higher social media usage ($\frac{\partial x_t^*}{\partial \Delta_t} > 0$), and this effect to be magnified by the size of an individual's social network ($\frac{\partial^2 x_t^*}{\partial X_t \partial \Delta_t} > 0$). In other words, β_3 and β_4 are tests to rule out cases of perfect present bias and projection bias.

The regression results presented in Table 4 largely align with the expectations and predictions of our theoretical model. The estimates indicate strong persistence in social media usage, with the coefficients on lagged usage ranging between 0.43 and 0.63 across all platforms. This suggests that past behavior is a strong predictor of current usage, reflecting habitual engagement with social media.

Table 4: App Usage Regression

	(1) Facebook	(2) Instagram	(3) Twitter	(4) Snapchat	(5) Browser	(6) YouTube
Own Lag Usage	0.727***	0.705***	0.790***	0.681***	0.716***	0.726***
	(0.00516)	(0.00481)	(0.00364)	(0.00407)	(0.00652)	(0.00531)
Distance Traveled	-3.438***	-0.654***	-0.216*	0.0194	-0.146	-0.984*
	(0.520)	(0.242)	(0.124)	(0.148)	(0.342)	(0.587)
SCI Weighted Usage	3.701***	1.736***	0.838***	0.883***	1.362***	2.216***
	(0.102)	(0.0639)	(0.0359)	(0.0368)	(0.0638)	(0.0769)
Weighted UsageXWeighted Mobility	0.0258*	0.0849***	0.0503***	-0.000860	0.0568***	-0.00650
	(0.0154)	(0.0126)	(0.00872)	(0.00804)	(0.0123)	(0.0127)
SCI Weighted Mobility	105.5***	29.51***	10.46***	12.48**	76.51***	53.76***
	(18.52)	(7.021)	(3.656)	(5.095)	(13.88)	(18.67)
Weighted UsageXDistance Traveled	-0.00282***	-0.00173***	-0.000847*	-0.0000529	-0.000504	-0.000986*
	(0.000465)	(0.000522)	(0.000483)	(0.000395)	(0.000326)	(0.000581)
Observations	115397	115397	115397	115397	115397	115397
Individual FE	Yes	Yes	Yes	Yes	Yes	Yes
R^2	0.22	0.26	0.39	0.34	0.11	0.21

Standard errors in parentheses

* $p < .1$, ** $p < .05$, *** $p < .01$

Consistent with the patterns observed in Table 2, the individual's distance traveled is negatively correlated with the usage of some, but not all, social media platforms. In particular, Snapchat usage appears largely unaffected by declines in individual mobility during lockdowns, whereas Facebook, Instagram, and YouTube exhibit stronger negative correlations. This suggests that reductions in mobility due to lockdown measures led to increased engagement with these platforms, while Snapchat usage remained relatively stable.

The estimates on SCI-weighted social media usage are uniformly positive and sta-

tistically significant, confirming the presence of network effects. Increased social media usage by an individual's friends is associated with greater usage by the individual, reinforcing the complementarity between social network activity and engagement with these platforms. An interesting finding is the differential impact of social network influence across platforms. While the standard deviation of Facebook's SCI-weighted usage is only about 5% higher than that of browser usage, the coefficient on Facebook's SCI-weighted usage is nearly three times as large (3.701 vs 1.362). Similarly, the standard deviation of Facebook's SCI-weighted usage is similar to that of YouTube's, but the coefficient on Facebook's SCI-weighted usage is 2/3 higher than that of YouTube's. This suggests that the social network effects of Facebook are substantially stronger than those of browsers and YouTube.

5.3 Persistence without Social Network

One of our key contributions is incorporating individual social network size into the analysis, distinguishing our approach from prior studies on digital addiction, such as Allcott, Gentzkow, and Song (2022). In Table 4, we show that social networks influence social media usage, as evidenced by the positive coefficient on SCI-weighted usage—higher usage within an individual's network is associated with higher own usage. In this section, we examine how omitting social network size affects estimated persistence in social media consumption.

Table 5 replicates the regression from Table 4 but excludes social network controls for Facebook. On top of the individual fixed effects with IV (columns 3 and 4) as in Table 4, we also use individual fixed effects without instrumenting the lagged usage (columns 3 and 4). In all the specifications with social network controls, the signs of the coefficients are consistent with those in Table 4, therefore mostly align with the expectations and predictions of our theoretical model.

Table 5: Apps Usage Regression with and without Social Network

	(1) Ind. FE	(2) Ind. FE	(3) IV (Usage Lag)	(4) IV (Usage Lag)
Own Lag Usage	0.500***	0.508***	0.727***	0.740***
	(0.00254)	(0.00253)	(0.00516)	(0.00514)
Distance Traveled	-3.869***	-1.724***	-3.438***	-1.385***
	(0.502)	(0.342)	(0.520)	(0.354)
SCI Weighted Usage	4.341***		3.701***	
	(0.0982)		(0.102)	
Weighted UsageXWeighted Mobility	0.0295**		0.0258*	
	(0.0149)		(0.0154)	
SCI Weighted Mobility	106.3***		105.5***	
	(17.90)		(18.52)	
Weighted UsageXDistance Traveled	-0.00300***		-0.00282***	
	(0.000450)		(0.000465)	
Observations	115397	117865	115397	117865
Individual FE	Yes	Yes	Yes	Yes

Standard errors in parentheses

* $p < .1$, ** $p < .05$, *** $p < .01$

Also, the results indicate slightly higher persistence in individual social media usage, as reflected in the increased coefficient on lagged own usage. This suggests that failing to account for social network size leads to a small but systematic overestimation of individual persistence in app engagement. These findings underscore the importance of incorporating network effects when studying digital addiction.

6 Conclusion

This paper examines how social networks shape social media addiction, distinguishing between true addiction and network-driven persistence. We develop a dynamic model incorporating rational addiction, behavioral biases, and peer effects, generating testable implications validated with a long-panel dataset.

Using individual app usage and mobility data combined with the Facebook Social Connectedness Index, we show that social media addiction is short-lived, with usage persistence dissipating within a year. Strong peer effects drive engagement, as individuals use more social media when their network does. Exploiting exogenous shocks from COVID-19 lockdowns, we find that reduced network-wide mobility lowers future engagement, reinforcing network-driven persistence. Our results reject strong behavioral biases,

emphasizing habit formation and network externalities.

By extending addiction models to include social networks, we provide new insights into digital consumption. If social media use generates network externalities, individuals may over-consume, justifying potential regulatory interventions such as usage caps, pricing adjustments, or nudges. Future research should explore how network structures influence addiction and whether targeted policies can mitigate overuse while preserving social benefits.

References

Allcott, Hunt, Luca Braghieri, Sarah Eichmeyer, and Matthew Gentzkow. 2020. "The Welfare Effects of Social Media." *American Economic Review* 110 (3):629–76. URL https://www.aeaweb.org/articles?id=10.1257/aer.20190658.

Allcott, Hunt, Matthew Gentzkow, and Lena Song. 2022. "Digital Addiction." *American Economic Review* 112 (7):2424–63. URL https://www.aeaweb.org/articles?id=10.1257/aer.20210867.

Bailey, Michael, Rachel Cao, Theresa Kuchler, Johannes Stroebel, and Arlene Wong. 2018. "Social Connectedness: Measurement, Determinants, and Effects." *Journal of Economic Perspectives* 32 (3):259–80. URL https://www.aeaweb.org/articles?id=10.1257/jep.32.3.259.

Becker, Gary S. and Kevin M. Murphy. 1988. "A Theory of Rational Addiction." *Journal of Political Economy* 96 (4):675–700. URL http://www.jstor.org/stable/1830469.

Bernheim, B. Douglas and Antonio Rangel. 2004. "Addiction and Cue-Triggered Decision Processes." *American Economic Review* 94 (5):1558–1590.

Gilo, David and Yevgeny Tsodikovich. 2020. "Addiction to a Network." URL https://papers.ssrn.com/sol3/papers.cfm?abstract_id=3580693. SSRN Working Paper No. 3580693.

Gruber, Jonathan and Botond Köszegi. 2001. "Is Addiction 'Rational'? Theory and Evidence." *The Quarterly Journal of Economics* 116 (4):1261–1303. URL http://www.jstor.org/stable/2696459.

Kwon, Hyeokkoo Eric, Hyunji So, Sang Pil Han, and Wonseok Oh. 2016. "Excessive Dependence on Mobile Social Apps: A Rational Addiction Perspective." *Information Systems Research* 27 (4):919–939. URL https://doi.org/10.1287/isre.2016.0658.

Laibson, David. 1997. "Golden Eggs and Hyperbolic Discounting." *The Quarterly Journal of Economics* 112 (2):443–477. URL http://www.jstor.org/stable/2951242.

Loewenstein, George, Ted O'Donoghue, and Matthew Rabin. 2003. "Projection Bias in Predicting Future Utility*." *The Quarterly Journal of Economics* 118 (4):1209–1248. URL https://doi.org/10.1162/003355303322552784.

O'Donoghue, Ted and Matthew Rabin. 1999. "Doing It Now or Later." *American Economic Review* 89 (1):103–124. URL https://www.aeaweb.org/articles?id=10.1257/aer.89.1.103.

Pew Research Center. 2024. "Teens, Social Media and Technology 2024." Available at: https://www.pewresearch.org/internet/2024/12/12/teens-social-media-and-technology-2024/.

Reif, Julian. 2019. "A MODEL OF ADDICTION AND SOCIAL INTERACTIONS." *Economic Inquiry* 57 (2):759–773. URL https://onlinelibrary.wiley.com/doi/abs/10.1111/ecin.12709.

Somasundaram, Jeeva, Laura Zimmermann, and Pham Quang Duc. 2020. "Leveraging Rational Addiction Theory to Reduce Mobile Usage." URL https://papers.ssrn.com/sol3/papers.cfm?abstract_id=3719413. SSRN Working Paper No. 3719413.

Appendix A Theory Appendix

Appendix A.1 Proof

Appendix A.1.1 Lemma 1

The optimal SN activities, $x_t = x_t^*$, that maximizes $U(S_0)$ are given by:

$$x_t^* = \arg\max_x \left\{-h(x+m) + \lambda(x,X)(u - p\Delta_t)\right\}, \tag{A1}$$

where Δ_t solves the following ordinary differential equation

$$\frac{d\Delta_t}{dt} = [r + \delta + p\lambda(x_t^*, X)]\Delta_t - k - h(\bar{x}) + h(x_t^* + m) - \lambda(x_t^*, X)u, \text{ where } \Delta_T = 0. \tag{A2}$$

Furthermore, we have

$$0 \leq \Delta_t < \frac{u}{p}. \tag{A3}$$

Proof. Note that it is straight-forward to verify that (2) and (3) solve the following HJB equations

$$\begin{aligned} rV_t^U &= \max_{x_t} \dot{V}_t^U - h(x_t + m_t) + \lambda(x_t, X_t)\left[u + p\left(V_t^A - V_t^U\right)\right], & \text{(A4)} \\ rV_t^A &= \dot{V}_t^A - k - h(\bar{x}) + \delta\left(V_t^U - V_t^A\right), & \text{(A5)} \end{aligned}$$

Thus, by substracting (2) from (3) we have established (5) of Lemma 1.

Note that it is straight-forward to verify that Δ_t of (5) also admits following integral form:

$$\Delta_t = \int_t^T e^{-\int_t^\tau [r+\delta+p\lambda(x_s^*,X)]ds}\left[k + h(\bar{x}) - h(x_\tau^* + m) + \lambda(x_\tau^*, X)u\right]d\tau. \tag{A6}$$

Since we have $h(\bar{x}) \geq h(x_\tau^* + m)$ for any x_τ^*, the integral is always positive, i.e., $\Delta_t \geq 0$.

Finally, to prove $\Delta_t < \frac{u}{p}$, suppose it is not the case. Since $\Delta_T = 0$, the premise implies that there exists τ with $\Delta_\tau = u/p$ and $\Delta_t < u/p$ for all $t > \tau$; otherwise if such τ does not exist then we must have $\Delta_t < u/p$ for all τ, violating the premise. Thus, we must have $\dot{\Delta}_\tau < 0$. Also, the fact that $\Delta_\tau = u/p$ implies $x_\tau^* = 0$. However, from (5) and assumption

(1), we have

$$\dot{\Delta}_\tau = (r+\delta)\frac{u}{p} - k - h(\bar{x}) + h(m) < 0,$$

which contradicts to the fact that $\dot{\Delta}_\tau < 0$. **QED**

Appendix A.1.2 Proposition 1

The comparative statics of the rational agent's activities and his marginal cost of addiction are

	Addiction prob. dp	Recovery rate $d\delta$	Addiction effect dk	Interaction benefit du	Matching efficiency $d\bar{\lambda}$
dx_t^*	$-$	$+$	$-$	$+$	$+$
$d\Delta_t$	$-$	$-$	$+$	$+$	$+$

Proof. Applying an envelope theorem on (5), we have

$$\frac{d^2\Delta_t}{dtdp} = [r+\delta+p\lambda(x_t^*,X)]\frac{d\Delta_t}{dp} + \lambda(x_t^*,X)\Delta_t.$$

It is straight-forward to verify that the above partial differential equation admits the following integral form:

$$\frac{d\Delta_t}{dp} = -\int_t^\infty e^{\int_t^\tau [r+\delta+p\lambda(x_s^*,X)]ds}\lambda(x_\tau^*,X)\Delta_\tau d\tau < 0.$$

Similarly, we have

$$\begin{aligned}
\frac{d\Delta_t}{d\delta} &= -\int_t^\infty e^{\int_t^\tau [r+\delta+p\lambda(x_s^*,X)]ds}\Delta_\tau d\tau < 0,\\
\frac{d\Delta_t}{dk} &= \int_t^\infty e^{\int_t^\tau [r+\delta+p\lambda(x_s^*,X)]ds}d\tau > 0,\\
\frac{d\Delta_t}{du} &= \int_t^\infty e^{\int_t^\tau [r+\delta+p\lambda(x_s^*,X)]ds}\lambda(x_\tau^*,X)\,d\tau > 0,\\
\frac{d\Delta_t}{d\bar{\lambda}} &= \frac{1}{\bar{\lambda}}\int_t^\infty e^{\int_t^\tau [r+\delta+p\lambda(x_s^*,X)]ds}\lambda(x_\tau^*,X)(u-p\Delta_\tau)\,d\tau > 0.
\end{aligned}$$

Finally, the first order condition w.r.t. x_t is given by

$$h'(x_t^*+m) = \lambda_x(x_t^*,X)(u-p\Delta_t). \tag{A7}$$

Differentiating the above, we have

$$\begin{aligned}
\frac{dx_t^*}{dp} &= \frac{-\lambda_x\left(x_t^*, X\right)\Delta_t}{h''\left(x_t^*+m\right)-\lambda_{xx}\left(x_t^*, X\right)\left(u-p\Delta_t\right)} < 0, \\
\frac{dx_t^*}{d\delta} &= \frac{-\lambda_x\left(x_t^*, X\right)p}{h''\left(x_t^*+m\right)-\lambda_{xx}\left(x_t^*, X\right)\left(u-p\Delta_t\right)}\frac{d\Delta_t}{d\delta} > 0, \\
\frac{dx_t^*}{dk} &= \frac{-\lambda_x\left(x_t^*, X\right)p}{h''\left(x_t^*+m\right)-\lambda_{xx}\left(x_t^*, X\right)\left(u-p\Delta_t\right)}\frac{d\Delta_t}{dk} < 0 \\
\frac{dx_t^*}{du} &= \frac{\lambda_x\left(x_t^*, X\right)}{h''\left(x_t^*+m\right)-\lambda_{xx}\left(x_t^*, X\right)\left(u-p\Delta_t\right)} > 0, \\
\frac{dx_t^*}{d\bar{\lambda}} &= \frac{\lambda_x\left(x_t^*, X\right)\left(u-p\Delta_t\right)}{\bar{\lambda}\left[h''\left(x_t^*+m\right)-\lambda_{xx}\left(x_t^*, X\right)\left(u-p\Delta_t\right)\right]} > 0.
\end{aligned}$$

QED

Appendix A.1.3 Proposition 2

The comparative statics of the behavioral agent's activities and his marginal value of addiction are

	Present bias $d\gamma$	Projection bias $d\alpha$	Perception bias $d\eta$
dx_t^*	$+$	$+$	$-$
$d\Delta_t^s$	$-$	0	$+$

Proof. Evaluating the first order condition of (7) at $x_t = \tilde{x}_{t,s}^*$, we solve $\tilde{x}_{t,s}^*$ as the solution to

$$\left[1-(1-\eta)\gamma\right]h'\left(\tilde{x}_{t,s}^*+m_{t+s}\right) = \lambda_x\left(\tilde{x}_{t,s}^*, X_{t+s}\right)\left(u-p\Delta_t^s\right). \tag{A8}$$

Differentiating the above, we have

$$\frac{d\tilde{x}_{t,s}^*}{d\gamma} = \frac{-p\lambda_x\left(\tilde{x}_{t,s}^*, X_{t+s}\right)}{h''\left(\tilde{x}_{t,s}^*+m_{t+s}\right)-\lambda_{xx}\left(\tilde{x}_{t,s}^*, X\right)\left(u-p\Delta_t^s\right)}\frac{d\Delta_t^s}{d\gamma}$$

Differentiating (8), we have

$$\begin{aligned}
\frac{d^2\Delta_t^s}{dsd\gamma} &= \left(r+\delta+p\tilde{\lambda}_{t,s}\right)\frac{d\Delta_t^s}{d\gamma} + \left[h''\left(\tilde{x}_{t,s}^*+m_{t+s}\right)-\lambda_{xx}\left(\tilde{x}_{t,s}^*, X_{t+s}\right)u\right]\frac{d\tilde{x}_{t,s}^*}{d\gamma}, \\
&= \left\{\left(r+\delta+p\tilde{\lambda}_{t,s}\right)-\frac{\left[h''\left(\tilde{x}_{t,s}^*+m_{t+s}\right)-\lambda_{xx}\left(\tilde{x}_{t,s}^*, X_{t+s}\right)u\right]p\lambda_x\left(\tilde{x}_{t,s}^*, X_{t+s}\right)}{h''\left(\tilde{x}_{t,s}^*+m_{t+s}\right)-\lambda_{xx}\left(\tilde{x}_{t,s}^*, X_{t+s}\right)\left(u-p\Delta_t^s\right)}\right\}\frac{d\Delta_t^s}{d\gamma}
\end{aligned} \tag{A9}$$

Define

$$D_{t,\tau}^{\gamma} \equiv \int_{\tau}^{T} \left\{ \left(r + \delta + p\tilde{\lambda}_{t,s} \right) - \frac{\left[h'' \left(\tilde{x}_{t,s}^{*} + m_{t+s} \right) - \lambda_{xx} \left(\tilde{x}_{t,s}^{*}, X_{t+s} \right) u \right] p\lambda_x \left(\tilde{x}_{t,s}^{*}, X_{t+s} \right)}{h'' \left(\tilde{x}_{t,s}^{*} + m_{t+s} \right) - \lambda_{xx} \left(\tilde{x}_{t,s}^{*}, X_{t+s} \right) (u - p\Delta_t^s)} \right\} ds.$$

Then we can verify that the partial differential equation (A9) admits the following closed-form solution:

$$\frac{d\Delta_t^s}{d\gamma} = -e^{-D_{t,s}^{\gamma}} > 0. \tag{A10}$$

Similarly, we can prove $\frac{d\Delta_t^s}{d\alpha} = 0$ and $\frac{d\Delta_t^s}{d\eta} > 0$.

Finally, evaluating the first order condition of (7) at $x_t = x_t^* \equiv x^* \left(X_t, \Delta_t^0; \gamma, \alpha \right)$, we solve $\tilde{x}_{t,s}^*$ as the solution to

$$(1 - \gamma) h' \left(x_t^* + m_{t+s} \right) = \lambda_x \left(x_t^*, X_t \right) \left[u - p \left(1 - \alpha \right) \Delta_t^0 \right]. \tag{A11}$$

differentiating the above, we have

$$\begin{aligned}
\frac{dx_t^*}{d\gamma} &= \frac{-p\lambda_x \left(x_t^*, X_t \right)}{h'' \left(x_t^* + m_t \right) - \lambda_{xx} \left(x_t^*, X \right) \left(u - p\Delta_t^0 \right)} \frac{d\Delta_t^0}{d\gamma} > 0, \\
\frac{dx_t^*}{d\alpha} &= \frac{p\lambda_x \left(x_t^*, X_t \right) \left(-\frac{d\Delta_t^0}{d\alpha} + \Delta_t^0 \right)}{h'' \left(x_t^* + m_t \right) - \lambda_{xx} \left(x_t^*, X \right) \left(u - p\Delta_t^0 \right)} > 0, \\
\frac{dx_t^*}{d\eta} &= \frac{-p\lambda_x \left(x_t^*, X_t \right)}{h'' \left(x_t^* + m_t \right) - \lambda_{xx} \left(x_t^*, X \right) \left(u - p\Delta_t^0 \right)} \frac{d\Delta_t^0}{d\eta} < 0.
\end{aligned}$$

QED

Appendix A.1.4 Proposition 3

$\Delta_{\varepsilon,t}^s$ solves the follow ODE

$$\frac{d\Delta_{\varepsilon,t}^s}{ds} = \left(r + \delta + p\tilde{\lambda}_t^s \right) \Delta_{\varepsilon,t}^s - \beta_s \left(u - p\Delta_{\varepsilon,t}^s \right) \left[\tilde{\lambda}_{X,t}^s - \frac{(1 - \eta)\gamma}{1 - (1 - \eta)\gamma} \tilde{\lambda}_{x,t}^s \frac{\partial x_{t,s}^*}{\partial X_{t+s}} \right],$$

where $\Delta_{\varepsilon,t}^{T-t} = 0$ and its solution is given by

$$\Delta_{\varepsilon,t}^0 = \int_0^{T-t} e^{-\int_0^s r + \delta + p\tilde{\lambda}_t^{\tau} d\tau} \beta_s \left(u - p\Delta_{\varepsilon,t}^s \right) \left[\tilde{\lambda}_{X,t}^s - \frac{(1 - \eta)\gamma}{1 - (1 - \eta)\gamma} \tilde{\lambda}_{x,t}^s \frac{\partial x_{t,s}^*}{\partial X_{t+s}} \right] ds.$$

Proof. Similar to the proof of Proposition 2.

Appendix A.1.5 Proposition 4

The comparative statics with respect to X_t, m_t and ε_t are given as follows:

a. $\frac{\partial x_t^*}{\partial X_t} = \lambda_{xX,t} / \left[\frac{(1-\gamma)h_t''}{u-p(1-\alpha)\Delta_t} - \lambda_{xx,t}\right]$;

b. $\frac{\partial x_t^*}{\partial m_t} = -1 / \left[\frac{1-\gamma}{u-p(1-\alpha)\Delta_t} - \theta_t\right]$;

c. $\frac{\partial^2 x_t^*}{\partial m_t \partial X_t} = -\left(\frac{\partial x_t^*}{\partial m_t}\right)^2 \left(\theta_{X,t} + \theta_{x,t}\frac{\partial x_t^*}{\partial X_t}\right)$;

d. $\frac{\partial x_t^*}{\partial \varepsilon_t} = -\frac{p(1-\alpha)\Delta_{\varepsilon,t}}{[u-p(1-\alpha)\Delta_t]^2}\frac{h_t'}{h_t''}\frac{\partial x_t^*}{\partial m_t}$;

e. $\frac{\partial^2 x_t^*}{\partial X_t \partial \varepsilon_t} = -\frac{p(1-\alpha)\Delta_{\varepsilon,t}}{[u-p(1-\alpha)\Delta_t]^2}\left[\frac{h_t'}{h_t''}\frac{\partial^2 x_t^*}{\partial m_t \partial X_t} + \frac{\partial h_t'/h_t''}{\partial x}\frac{\partial x_t^*}{\partial X_t}\frac{\partial x_t^*}{\partial m_t}\right]$,

where $\theta_t \equiv \frac{\lambda_{xx}(x,X_t)}{h''(x+m_t)} < 0$, $\theta_{X,t} \equiv \frac{\partial \theta_t}{\partial X} = \frac{\lambda_{xxX,t}}{\lambda_{xx,t}}\theta_t \leq 0$ *and* $\theta_{x,t} \equiv \frac{\partial \theta_t}{\partial x} \geq 0$.

Proof. Established after differentiating the first order condition of (7) w.r.t the related variables.

Appendix A.2 Extension

Appendix A.2.1 Other factors

Suppose m_t and X_t are time-varying. Note that (2) and (3) solve the following HJB equations

$$\begin{aligned} rV_t^U &= \max_{x_t} \dot{V}_t^U - h(x_t + m_t) + \lambda(x_t, X_t)\left[u + p\left(V_t^A - V_t^U\right)\right], \\ rV_t^A &= \dot{V}_t^A - k - h(\bar{x}) + \delta\left(V_t^U - V_t^A\right). \end{aligned}$$

The ODE for the cost of addition becomes

$$\frac{d\Delta_t}{dt} = \left[r + \delta + p\lambda(x_t^*, X_t)\right]\Delta_t - k - h(\bar{x}) + h(x_t^* + m_t) - \lambda(x_t^*, X_t)\,u, \text{ where } \Delta_T = 0.$$

The choice of the rational agent becomes

$$x_t^* = \arg\max_x \left\{-h(x + m_t) + \lambda(x, X_t)(u - p\Delta_t)\right\}.$$

Appendix A.2.2 Activity choice of the addicted

Suppose addicted agents can choose the intensity of social activities, y_t, and enjoy $u^a > u$ from the social connection. The values of being non-addicted and addicted become

$$\begin{aligned} rV_t^U &= \max_{x_t} \dot{V}_t^U - h\left(x_t + m\right) + \lambda\left(x_t, X\right)\left[u + p\left(V_t^A - V_t^U\right)\right], \\ rV_t^A &= \max_{y_t} \dot{V}_t^A - k - h\left(y_t + m\right) + \lambda\left(y_t, X\right)u^a + \delta\left(V_t^U - V_t^A\right), \end{aligned}$$

The choice of the addicted agent becomes

$$\begin{aligned} y_t^* &= \arg\max_x \left\{-h\left(y + m\right) + \lambda\left(y, X\right)u^a\right\}, \\ &> x_t^* = \arg\max_x \left\{-h\left(x + m\right) + \lambda\left(x, X\right)\left(u - p\Delta_t\right)\right\}. \end{aligned}$$

The ODE for the cost of addition becomes

$$\frac{d\Delta_t}{dt} = \left[r + \delta + p\lambda\left(x_t^*, X_t\right)\right]\Delta_t - k - h\left(y_t^* + m\right) + h\left(x_t^* + m\right) + \lambda\left(y_t^*, X_t\right)u^a - \lambda\left(x_t^*, X_t\right)u, \text{ where } \Delta_T = 0$$

Appendix A.2.3 Cold turkey

Suppose addicted agents can vary $\delta = \delta\left(c_t\right)$ by choosing the intensity of "cold turkey", c_t, where $\delta\left(c_t\right)$ is increasing in c_t. Cold turkey requires agents' effort by entering h. The values of being non-addicted and addicted become

$$\begin{aligned} rV_t^U &= \max_{x_t} \dot{V}_t^U - h\left(x_t + m\right) + \lambda\left(x_t, X\right)\left[u + p\left(V_t^A - V_t^U\right)\right], \\ rV_t^A &= \max_{y_t} \dot{V}_t^A - k - h\left(c_t + m\right) + \delta\left(c_t\right)\left(V_t^U - V_t^A\right), \end{aligned}$$

The choice of cold turkey is given by

$$c_t^* = \arg\max_c \left\{-h\left(c + m\right) + \delta\left(c\right)\Delta_t\right\}.$$

The ODE for the cost of addition becomes

$$\frac{d\Delta_t}{dt} = \left[r + \delta\left(c^*\right) + p\lambda\left(x_t^*, X_t\right)\right]\Delta_t - k - h\left(c_t^* + m\right) + h\left(x_t^* + m\right) - \lambda\left(x_t^*, X_t\right)u, \text{ where } \Delta_T = 0.$$

Appendix A.2.4 Multiple addiction states

Suppose addiction is measured by $S_t \in \{0, 1, 2, ..., A\}$, where A now is the maximal addiction state. The welfare cost of addiction $k(S_t)$ is increasing in S_t and the utility of social connection $u(S_t)$ is also increasing in S_t. When agents increase their social activity, it increases the probability of heightening their addiction state by an increment of one. Similar to the before, agents' addiction state will be reduced by an decrement of one at the rate δ. The values of agent with addiction S_t become

$$\begin{aligned} rV_t^S &= \max_{x_{S,t}} \dot{V}_t^S - k(S) - h(x_{S,t} + m) + \lambda(x_{S,t}, X)\left[u(S) + p\left(V_t^{S+1} - V_t^S\right)\right] + \delta\left(V_t^{S-1} - V_t^S\right) I(S \\ rV_t^A &= \dot{V}_t^S - k(A) - h(\bar{x}) + \delta\left(V_t^{A-1} - V_t^A\right). \end{aligned}$$

Define the marginal cost of addiction $S_t \leq A - 1$ as

$$\Delta_{S,t} \equiv V_t^S - V_t^{S+1}.$$

The activity choice of the agent becomes

$$x_{S,t}^* = \arg\max_x \left\{-h(x + m) + \lambda(x, X)\left(u(S) - p\Delta_{S,t}\right)\right\}.$$

The ODE for the marginal cost of addition is

$$\begin{aligned} \frac{d\Delta_{S,t}}{dt} &= \begin{cases} [r + \delta + p\lambda(\Delta_{S,t}, X)]\Delta_{S,t} - \delta\Delta_{S-1,t} - k(S) + k(S+1) - h\left(x_{S+1,t}^* + m\right) \\ +h\left(x_{S,t}^* + m\right) + \lambda\left(x_{S+1,t}^*, X_t\right)u(S+1) - \lambda\left(x_{S,t}^*, X_t\right)u(S) \end{cases}, \text{ for } S \in \{1 \\ \frac{d\Delta_{S,t}}{dt} &= \begin{cases} [r + \delta + p\lambda(\Delta_{A-1,t}, X)]\Delta_{A-1,t} - \delta\Delta_{A-2,t} - k(A-1) + k(A) - h(\bar{x} + m) \\ +h\left(x_{A-1,t}^* + m\right) - \lambda\left(x_{A-1,t}^*, X_t\right)u(A-1) \end{cases}, \text{ for } S = A \\ \frac{d\Delta_{S,t}}{dt} &= \begin{cases} [r + \delta + p\lambda(\Delta_{0,t}, X)]\Delta_{0,t} - k(0) + k(1) - h\left(x_{1,t}^* + m\right) \\ +h\left(x_{0,t}^* + m\right) + \lambda\left(x_{1,t}^*, X_t\right)u(1) - \lambda\left(x_{0,t}^*, X_t\right)u(0) \end{cases}, \text{ for } S = 0, \end{aligned}$$

where $\Delta_{S,T} = 0$.

Appendix A.2.5 Making friends

Suppose friends are either addicted with activity $\bar{x}$ or non-addicted with activity x_t^*. To keep the environment simple, assume each agent has almost one friend, but his friend can become addicted or non-addicted over time,. The agent could lose his friend at the rate ψ_L but gain a new friend at the rate ψ_G, where with probability π^A his new friend is addicted. Thus, the state of X_t is $X_t \in \{0, x_t^*, \bar{x}\}$. The values of being non-addicted and addicted become

$$\begin{aligned} rV_{X,t}^U &= \max_{x_{X,t}} \dot{V}_{X,t}^U - h\left(x_{X,t}+m\right) + \lambda\left(x_{X,t}, X\right)\left[u + p\left(V_{X,t}^A - V_{X,t}^U\right) + 1_{X=x_t^*} p\left(V_{\bar{x},t}^U - V_{X,t}^U\right)\right] \\ &\quad + 1_{X=0}\psi_G\left(\pi^A V_{\bar{x},t}^U + \pi^U V_{x_t^*,t}^U - V_{X,t}^U\right) + 1_{X=x_t^*}\psi_L\left(V_{0,t}^U - V_{X,t}^U\right) + 1_{X=\bar{x}}\delta\left(V_{x_t^*,t}^U - V_{X,t}^U\right) \\ rV_{X,t}^A &= \max_{y_t} \dot{V}_t^A - k - h\left(\bar{x}\right) + \delta\left(V_{X,t}^U - V_{X,t}^A\right). \end{aligned}$$

Appendix A.2.6 Network competition

Suppose there are N networks availble where his friend's activity on network $n \in \{1, 2, ..., N\}$ is X_n. Networks can vary in quality and addictiveness such that the utility of social connection on network n is given by u^n, and the probability of becoming addiction is given by p^n. The values of being non-addicted becomes

$$\begin{aligned} rV_t^U &= \max_{\{x_{n,t}\}} \dot{V}_t^U - h\left(\sum_n x_{n,t} + m\right) + \sum_n \lambda\left(x_{n,t}, X_n\right)\left[u^n + p^n\left(V_t^A - V_t^U\right)\right], \\ rV_t^A &= \max_{y_t} \dot{V}_t^A - k - h\left(\bar{x}\right) + \delta\left(V_t^U - V_t^A\right), \end{aligned}$$

The choice of the agent's activity on network n becomes

$$x_{n,t}^* = \arg\max_{x_{n,t}} \left\{ -h\left(\sum_n x_{n,t} + m\right) + \lambda\left(x_{n,t}, X_n\right)\left(u^n - p^n \Delta_t\right) \right\}.$$

The ODE for the cost of addition becomes

$$\frac{d\Delta_t}{dt} = \left[r + \delta + p\sum_n \lambda\left(x_{n,t}^*, X_n\right)\right]\Delta_t - k - h\left(\bar{x}\right) + h\left(\sum_n x_{n,t}^* + m\right) - \sum_n \lambda\left(x_{n,t}^*, X_n\right) u^n, \text{ where } \Delta_T = 0.$$

Appendix B Apps Usage Regression by Age Group (FB and IG)

To explore heterogeneity in social media usage, we re-estimate the regression for Facebook and Instagram across different age groups. Facebook is more popular among individuals over 30, while Instagram is favored by those under 30. This analysis allows us to examine whether behavior differs across these demographic segments.

The first four columns of Table A1 present results for Facebook across different age groups, while the last four columns report findings for Instagram. The results largely align with the main findings in Table 4, supporting the testable implications of our rational addiction model.

Table A1: Apps Usage Regression by Age Group (FB and IG)

	Facebook				Instagram			
	Below 30	30-45	46-60	Above 60	Below 30	30-45	46-60	Above 60
Own Lag Usage	0.508***	0.491***	0.502***	0.526***	0.543***	0.501***	0.506***	0.370***
	(0.00551)	(0.00390)	(0.00499)	(0.00779)	(0.00531)	(0.00396)	(0.00506)	(0.00867)
Distance Traveled	-1.229	-4.399***	-10.51***	-15.17***	-0.359	-1.130***	-0.638*	-0.407
	(0.759)	(0.704)	(2.116)	(3.886)	(0.614)	(0.413)	(0.377)	(0.568)
SCI Weighted Usage	2.836***	4.890***	4.906***	2.069***	5.923***	2.112***	0.190***	0.137*
	(0.198)	(0.152)	(0.196)	(0.321)	(0.221)	(0.0943)	(0.0558)	(0.0827)
Weighted Usage	0.0801**	0.0551**	-0.0620**	0.156***	0.367***	0.0701***	0.00220	-0.000320
XWeighted Mobility	(0.0315)	(0.0233)	(0.0290)	(0.0460)	(0.0389)	(0.0186)	(0.0123)	(0.0155)
SCI Weighted Mobility	39.09	153.0***	83.03**	107.2**	79.05***	28.65***	0.0375	9.052
	(32.45)	(28.76)	(37.59)	(51.82)	(23.36)	(10.22)	(6.840)	(7.889)
Weighted Usage	-0.000308	-0.00349***	-0.0107***	0.00690	-0.00375***	-0.00265***	0.0000797	-0.000873
XDistance Traveled	(0.000940)	(0.000601)	(0.00278)	(0.00502)	(0.00121)	(0.000903)	(0.000903)	(0.000977)
Constant	-2811.1***	1369.7***	322.3***	-774.3***	1716.9***	119.5***	-1008.8***	-1627.2***
	(69.93)	(56.37)	(71.44)	(102.7)	(51.58)	(20.80)	(17.49)	(27.91)
Observations	24468	49229	29961	11739	24468	49229	29961	11739
Individual FE	Yes	Yes	Yes	Yes	Yes	Yes	Yes	Yes
R^2	0.86	0.84	0.83	0.85	0.83	0.83	0.78	0.75

Standard errors in parentheses

* $p < .1$, ** $p < .05$, *** $p < .01$

When splitting the sample by age, we find that network effects for Facebook are strongest among individuals aged 30–60, the demographic that engages most intensively with the platform. Conversely, network effects for Instagram are most pronounced among those under 30, reflecting their greater engagement with the app. These patterns are consistent with platform-specific usage trends and reinforce the role of social networks in

shaping digital consumption behavior.